

Enhanced photodegradation of di(2-ethyl)hexyl phthalate by Molecularly Imprinted titanium dioxide

Yu Shi¹, Fang-yan Chen^{*1}, Li-na He¹, Yu-bin Tang^{1,2}

¹School of Environmental and Chemical Engineering, Jiangsu University of Science and Technology, Zhenjiang, China

²Zhangjiagang Industrial Technology Research Institute, Jiangsu University of Science and Technology, Zhangjiagang, China

Abstract. To enhance the photocatalytic degradation efficiency and selectivity of di(2-ethyl)hexyl phthalate (DEHP), molecularly imprinted TiO₂ (MIP-TiO₂) was synthesized with di(2-ethylhexyl) phthalate as template molecule. The as-prepared MIP-TiO₂ was characterized by Field emission scanning electron microscopy (SEM), X-ray diffraction (XRD), Fourier infrared spectroscopy (FI-IR), UV-Visible diffuse reflection spectroscopy (UV-Vis) and photoluminescence spectroscopy (PL). The selective adsorption and photocatalytic activity of MIP-TiO₂ for DEHP were studied. The results show that DEHP molecularly imprinted polymer was coated on the surface of TiO₂. The light-response of MIP-TiO₂ was broadened. The photo-generated electron/hole recombination on the surface of TiO₂ decreased. The selective recognition to DEHP was improved. Compared with TiO₂, MIP-TiO₂ exhibited higher photocatalytic activity and selectivity to DEHP. The photocatalytic degradation efficiency of DEHP (5mg/L) by MIP-TiO₂ was 89%. The photocatalytic degradation rate of DEHP by MIP-TiO₂ is 1.5 times that by TiO₂. MIP-TiO₂ could be reused.

1 Introduction

Phthalate (PAEs) is a kind of widely used plasticizer, which can increase the flexibility, plasticity and mechanical strength of plastics. PAEs combine with monomer molecule of plastic via hydrogen bonds or van der Waals forces, so they can easily migrate from plastic matrix into the environment [1-3]. As one of the most common PAEs, di(2-ethylhexyl) phthalate (DEHP) has been detected in soil, water and food around the world, and has been considered as an environmental priority pollutant in some countries [4,5]. DEHP has obvious male reproductive toxicity, which can cause testicular dysplasia, cryptorchidism, decreased sperm quality and potential threats to human liver metabolism [6-8]. Therefore, it is significant how to rapidly degrade DEHP in wastewater or environment.

The photocatalytic oxidation has attracted increasing attention due to their advantages of high efficiency and thorough degradation of pollutants [9]. TiO₂ is a commonly used photocatalyst because of non-toxicity, high efficiency and optical stability [10, 11]. However, TiO₂ is lack of selectivity for photocatalytic degradation of organic pollutants, resulting in preferential degradation of other high-concentration organic

substances coexisting in wastewater, while low-concentration target pollutants that need to be removed are not effectively degraded [12,13]. Therefore, in order to improve the photocatalytic degradation efficiency of toxic organic pollutants with low concentrations in wastewater, it is of great significance to develop photocatalysts with high selectivity for the degradation of target pollutants. Molecularly imprinted polymers have well-matched pores and adsorption sites which can specifically recognize template molecules or molecules with similar structures, and have been widely used in chromatographic separation, solid phase extraction, sensors and other fields. In recent years, it has been found that the combination of photocatalytic technology and molecular imprinting can effectively improve the photocatalytic efficiency and selectivity of the catalyst for target pollutants [14-17]. A lot of molecularly imprinted TiO₂ have been reported in degradation of some organic pollutants [14-18]. However, the molecularly imprinted TiO₂ with DEHP as template molecule has not been reported. In addition, there are few reports on the effect mechanism of molecular imprinting modification on the photocatalytic performance of the catalyst.

In present work, a molecularly imprinted TiO₂ was synthesized with DEHP as template molecule. The selectively photocatalytic degradation of DEHP by

*1Corresponding author: catchen1029@sohu.com

molecularly imprinted TiO_2 was investigated. The mechanism of molecular imprinting to improve photocatalytic performance was discussed, which provided basis for the development of photocatalysts with high selectivity.

2. Experimental

2.1 Materials

Titanium sulphate, ethylenediamine tetraacetic acid, urea, di(2-ethylhexyl) phthalate (DEHP), Dibutyl phthalate (DBP), dimethyl phthalate(DMP), methacrylic acid (MAA), ethylene glycol dimethacrylate (EGDMA), azobisisobutyronitrile (AIBN), acetic acid, absolute ethanol, and methanol were purchased from Sinopharm Chemical Reagent Co., Ltd. Titanium sulphate is of chemical grade. Methanol is chromatographically pure. The other reagents are of analytical grade.

2.2 Preparation of MIP-TiO₂

MIP-TiO₂ was synthesized by microwave heating reaction method. Titanium sulfate (3.6 g) was dissolved in 250 mL of distilled water under vigorous agitation, and then ethylene diamine tetraacetic acid (5.6 g) and urea (2.1 g) were added into the solutions. After being fully stirred, the solution was transferred to the Teflon-lined reactor and heated by microwave for 8 min. The resulting solid phase was centrifugally separated, and then washed with distilled water and anhydrous ethanol in turn. Finally, the solid was dried at 80°C in vacuum. White powder TiO₂ was obtained.

DEHP (1 mmol) was dissolved in 80 mL of ethanol in a three-necked flask, MAA (4 mmol) was added into the flask, and then stirred at room temperature for 3 h. TiO₂ (0.1 g) was added into the flask and dispersed under ultrasound, afterwards, EGDMA (10 mmol) and AIBN (0.02 g) were successively added into the flask. The mixture in the flask reacted at 60 °C under the nitrogen protection for 18 h. The product was washed with anhydrous ethanol, methanol/acetic acid and distilled water, respectively, dried in a vacuum at 60° C, and the white powder MIP-TiO₂ was obtained.

2.3 Photocatalytic experiments

MIP-TiO₂ (0.018 g) was dispersed in 30 mL DEHP solution with the concentration of 5 mg/L in a glass reactor, and the suspension were magnetically stirred for 30min in dark. Then, a 300 W ultraviolet lamp was turned on to illuminate the suspension. Samples were taken out for every 0.5 h. The concentration of DEHP was determined by high performance liquid chromatography and the degradation efficiency was calculated as eq. (1).

$$\eta = \frac{C_0 - C_t}{C_0} \times 100\% \quad (1)$$

Where, C_0 and C_t are the initial concentration of DEHP and the residual concentration after being illuminated for t h, respectively.

2.4 Determination of DEHP

The concentration of DEHP was determined by high performance liquid chromatograph (LC-20A Ultrafast LC, Shimadzu Japan) with an Inertsil ODS-SP C18 column (250 mm×4.6 mm×5 μm). The column temperature was 40°C, and the mobile phase was methanol/water (95:5, V/V) with a flow rate of 0.5 mL/min. The wavelength of the UV detector was 228 nm.

3 Results and discussion

3.1 Characterization of MIP-TiO₂

3.1.1 FT-IR spectra

FT-IR spectra of MIP-TiO₂ and TiO₂ are shown in Fig. 1. As given in spectrum of TiO₂ (Fig.1a), the strong absorption peak that appears between 500 and 750 cm⁻¹ corresponded to Ti-O bond. The absorption peaks at 3440 cm⁻¹ and 1620 cm⁻¹ was due to the stretching vibration and the bending vibration of the hydroxyl group from water molecular, respectively, indicating that bound moisture was adsorbed on the surface of TiO₂ samples. In spectrum of MIP-TiO₂ (Fig.1b), the adsorption band at 3443 cm⁻¹ and 957 cm⁻¹ are characteristic absorption peaks of -OH. The peaks at 2972 cm⁻¹, 1461 cm⁻¹ and 1382 cm⁻¹ belonged to the stretching vibration of -CH₂ in the polymer skeleton. The peak at 1259 cm⁻¹ was attributed to the stretching vibration absorption of the ester bonds in the crosslinker EGDMA. The peaks at 1074 cm⁻¹ and 1746 cm⁻¹ was assigned to C=O and C-O bonds, respectively [20, 21]. It is concluded that crosslinking polymerization occurred on the surface of TiO₂, and molecularly imprinted polymers were successfully synthesized.

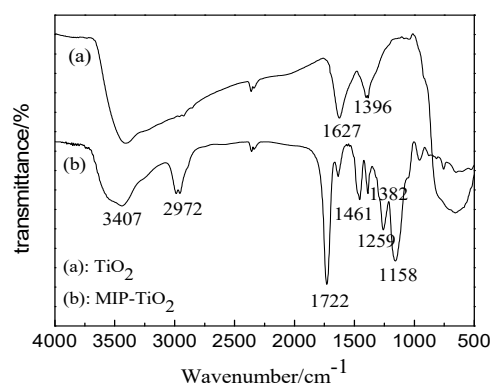


Fig. 1. FT-IR spectra of TiO₂ (a) and MIP-TiO₂ (b)

3.1.2 SEM

The SEM images of MIP-TiO₂ and TiO₂ are shown in Fig. 2. As seen from Fig. 2(a), the TiO₂ particles obtained are spherical, with particle sizes ranging from 200 to 300 nm. The particle size distribution is relatively uniform, but the surface is relatively rough. In Fig. 2(b), the

surface of the MIP-TiO₂ particles was smooth and flat, demonstrating that the molecularly imprinted polymer was successfully coated on the TiO₂ surface.

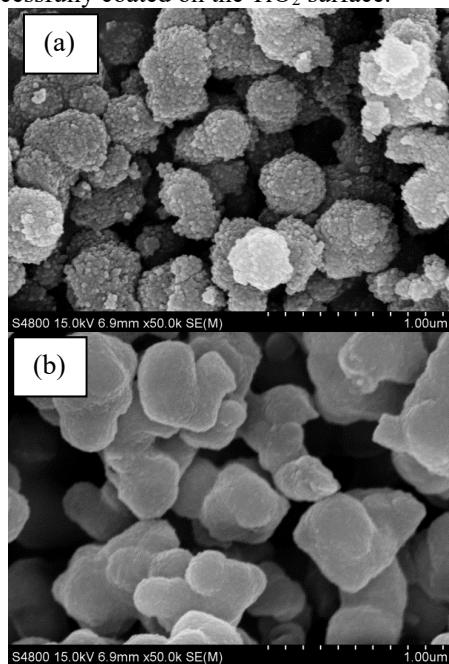


Fig. 2. SEM images of TiO₂ (a) and MIP-TiO₂ (b).

3.1.3 XRD analysis

Fig. 3 shows the XRD patterns of TiO₂ and MIP-TiO₂. It can be seen from Fig.3 (a) that the diffraction peaks at 2θ=25.3°, 38.1°, 48°, 54.2°, 55.4° and 63° can be assigned to (101), (004), (200), (105), (211) and (204) crystal planes of anatase TiO₂, indicating that the sample prepared is anatase TiO₂. The photocatalytic ability of anatase TiO₂ is obviously stronger than that of rutile or amorphous TiO₂, so, the TiO₂ sample prepared by macrowave method has strong photocatalytic ability for degradation of target substances [19]. Fig. 3(b) shows that MIP-TiO₂ has the same diffraction peaks as TiO₂. It is indicated that MIP-TiO₂ still maintains perfect anatase structure.

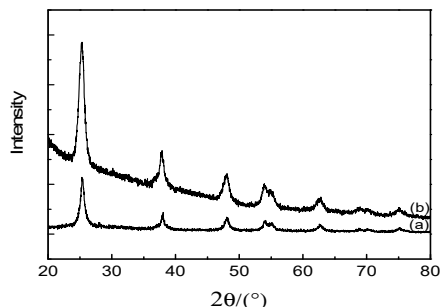


Fig. 3. XRD patterns of TiO₂ (a) and MIP-TiO₂ (b)

3.1.4 UV-vis diffuse reflection spectra

UV-vis of MIP-TiO₂ and TiO₂ are given in Fig.4. As shown in Fig. 4, compared with TiO₂, MIP-TiO₂ has stronger light absorption in the entire visible region. This is because the introduction of reactive groups to the

surface of TiO₂ during molecularly imprinted polymerization improves the light absorption performance of the catalyst [16]. The band gaps energy of catalysts can be estimated by eq. (2) [22].

$$E_g = \frac{hc}{\lambda_g} \quad (2)$$

Where, E_g is the band gap energy, h is the Planck's constant, C (m/s) is the speed of light, and λ_g is the absorption wavelength (nm).

According to eq. (2), the band gaps energy of TiO₂ and MIP-TiO₂ was calculated as 3.04 eV and 2.91 eV, respectively. MIP-TiO₂ has a narrow band gap, which can generate more electron-hole under light irradiation. It is suggested that MIP-TiO₂ would exhibit higher photocatalytic activity than TiO₂.

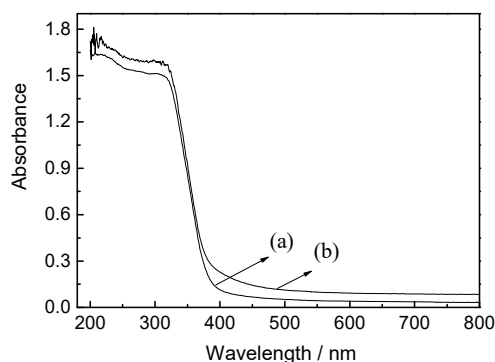


Fig. 4. UV-vis spectra of TiO₂ (a) and MIP-TiO₂ (b)

3.1.5 Photoluminescence (PL) spectra

Photoluminescence is widely used to assess the recombination probability of electron-hole pairs. Fig.5 shows the PL spectra of TiO₂ and MIP-TiO₂. It can be seen from Fig. 6 that the PL intensity of MIP-TiO₂ decreased significantly, compared to TiO₂. It is indicated that the molecularly imprinted polymer effectively inhibited the recombination of photo-generated electron/hole on the surface of TiO₂, which would be beneficial to improve the photocatalytic activity of MIP-TiO₂.

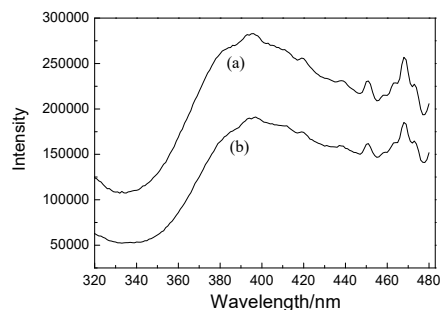


Fig. 5. PL spectra of TiO₂ (a) and MIP-TiO₂ (b)

3.2 Adsorption properties of MIP-TiO₂ for DEHP

The adsorption performance of the target pollutant on the catalyst directly affects the photocatalytic activity. In order to investigate the adsorption performance of MIP-

TiO₂ for DEHP, the adsorption rate and adsorption selectivity of MIP-TiO₂ to DEHP were determined.

3.2.1 Adsorption rate curve of DEHP onto MIP-TiO₂

The adsorption rate curve of DEHP onto MIP-TiO₂ is depicted in Fig. 6. As shown in Fig.6, the adsorption of DEHP onto TiO₂ and MIP-TiO₂ reaches adsorption equilibrium after 30 min, but the equilibrium adsorption capacity of DEHP onto MIP-TiO₂ is significantly higher than that onto TiO₂. This is because there is a binding site on the molecularly imprinted layer on the surface of MIP-TiO₂ that matches the target molecule DEHP, which greatly increases the adsorption capacity of DEHP. It is implied that MIP-TiO₂ have stronger photocatalytic degradation ability.

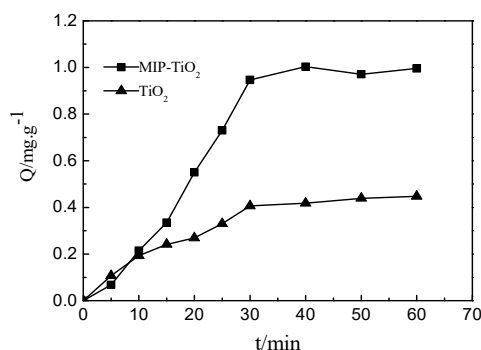


Fig. 6. curves of Adsorption rate MIP-TiO₂ and TiO₂ for DEHP

3.2.2 Adsorption selectivity of MIP-TiO₂ for DEHP

In order to investigate the selective recognition ability of MIP-TiO₂ to DEHP, MIP-TiO₂ and TiO₂ were used to adsorb DEHP and its analogs DBP and DMP with initial concentration of 5 mg/L, and the equilibrium adsorption amount is given in Fig. 7. As shown in Fig. 7, the adsorption capacities of DEHP and its analogs DBP and DMP on TiO₂ is lower than that on MIP-TiO₂, and the difference in adsorption capacity of the three pollutants is very small, indicating that TiO₂ has no selectivity to DEHP. While, the adsorption capacity of DEHP onto MIP-TiO₂ is significantly larger than that of DBP and DMP, and is obviously higher than that onto TiO₂, indicating that MIP-TiO₂ can specifically recognize DEHP molecules. This specific recognition not only can

enhance the adsorption capacity of DEHP on the catalyst surface and thus enhance the photocatalytic effect; but also can greatly enhance photocatalytic selectivity of MIP-TiO₂ to the target molecule DEHP.

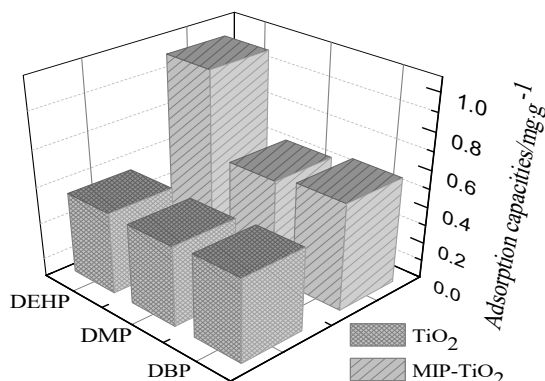


Fig. 7. Adsorption of DEHP and its analogues onto MIP-TiO₂

The imprinting factor (α) and the adsorption selectivity coefficient (β), which can be calculated by formulas (4) and (5), respectively [23], are usually used to evaluate adsorption selectivity of molecularly imprinted polymer to template molecules.

$$k = \frac{Q_e}{C_e} \quad (3)$$

$$\alpha = \frac{K_{MIP-TiO_2}}{K_{TiO_2}} \quad (4)$$

$$\beta = \frac{\alpha_{DEHP}}{\alpha_i} \quad (5)$$

Where, Q_e is equilibrium adsorption capacity (mg/g) of the target molecules onto the two catalysts, C_e is the concentration of DEHP (mg/L) at the adsorption equilibrium, α_{DEHP} is the imprinting factor of DEHP, and α_i is the imprinting factor of DBP or DMP.

According to formula (4) and (5), the imprinted factor of MIP-TiO₂ to DEHP, DBP and DMP and selectivity coefficients of MIP-TiO₂ to DEHP were calculated and listed in table 1. It can be seen from table 1 that the imprinting factor of MIP-TiO₂ to DEHP is significantly larger than that to DBP and DMP, and the selectivity coefficients of MIP-TiO₂ to DBP and DMP is 2.92 and 3.01, respectively.

Table 1. Adsorption selectivity of the MIP-TiO₂

Analytes	$Q_{MIP-TiO_2}$ (mg/g)	Q_{TiO_2} (mg/g)	$K_{MIP-TiO_2}$ (L/g)	K_{TiO_2} (L/g)	α	β
DBP	0.585	0.457	0.119	0.092	1.30	2.92
DMP	0.548	0.439	0.111	0.088	1.26	3.01
DEHP	0.995	0.448	0.449	0.118	3.79	-

3.3 Photocatalytic degradation of DEHP

The photocatalytic degradation efficiencies of DEHP are given in Fig.8. As seen in Fig. 8, the photodegradation efficiency of DEHP by MIP-TiO₂ is

significantly higher than that TiO₂. Within 180min, DEHP can be degraded 89% by MIP-TiO₂.

The photodegradation process of pullutants is generally simulated by the first-order kinetics as eq.(6) [24].

$$\ln\left(\frac{C_0}{C_t}\right) = kt \quad (6)$$

Where, C_0 is initial concentration of pollutant in solution. C_t is the concentration of pollutant solution at time t . k can be regarded as an apparent rate constant, the photocatalytic degradation ability of the catalyst can be known by k value.

The experimental data shown in Fig. 8 was fitted by the first-order kinetics model and the results are shown in table 2.

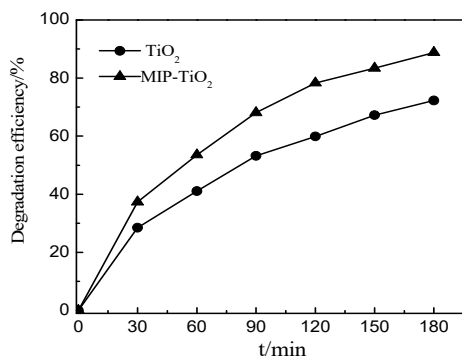


Fig. 8. Photocatalytic degradation rate of DEHP by MiP-TiO₂ and TiO₂

Table 2. Kinetics parameters for photocatalytic degradation of DEHP

Catalyst	k (min ⁻¹)	Correlation coefficient R^2
MIP-TiO ₂	0.0116	0.9917
TiO ₂	0.0079	0.979

As given in table 2, the correlation coefficients more than 0.97 suggested that photocatalytic degradation of DEHP by MIP-TiO₂ and TiO₂ can be simulated by the first-order kinetics. Moreover, the value of k indicated the degradation rate of DEHP by MIP-TiO₂ is 1.5 times that by TiO₂.

3.4 Photocatalytic selectivity of MIP-TiO₂ for DEHP

In order to investigate the selectivity of photocatalytic degradation of MIP-TiO₂ for DEHP, the photocatalytic degradation reactions of DEHP, DBP and DMP by MIP-TiO₂ and TiO₂ were carried out under the same conditions. The results were shown in Fig. 9. As given in Fig. 9 that the degradation efficiency of DBP by MIP-TiO₂ and TiO₂ is basically similar to each other, and only 67%. At the preliminary stage, the degradation efficiency

of DMP by MIP-TiO₂ was slightly higher than that by TiO₂, but after 3 h, the degradation efficiency of DMP by MIP-TiO₂ was identical to the degradation efficiency of DMP by TiO₂, which was about 60%. These results indicate that MIP-TiO₂ has no selectivity for photocatalysis of DBP and DMP. The degradation efficiency of DEHP by MIP-TiO₂ is 89%, far higher than that of DBP (67%) and DMP (61%).

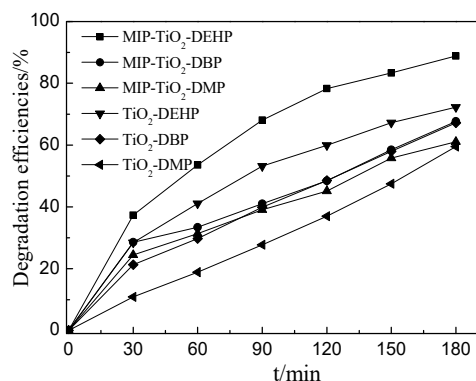


Fig. 9. The degradation rate of MIP-TiO₂ over different target

The data shown in Fig. 9 was fitted by equation (6) to obtain the photocatalytic degradation rate constants of DEHP, DBP and DMP by MIP-TiO₂ and TiO₂ and the results are listed in table 3.

The photocatalytic selectivity of MIP-TiO₂ to the template molecule can be expressed by a selectivity coefficient. The selectivity coefficient can be calculated according to eq. (7) and the results are also listed in table 3.

$$\alpha = \frac{R_{template}}{R_{analogue}} \quad (7)$$

$$R = \frac{k_M}{k_T} \quad (8)$$

Where, $R_{template}$ is ratio of photocatalytic degradation rate constant of template molecule by MIP-TiO₂ and TiO₂, calculated by formula (8). $R_{analogue}$ is ratio of photocatalytic degradation rate constant of analogs DBP and DMP by MIP-TiO₂ and TiO₂.

As listed in table 3, the selectivity coefficient of DEHP relative to DBP and DMP is 1.52 and 1.44, respectively. It is indicated that MIP-TiO₂ exhibits excellently photocatalytic selectivity to DEHP, and can degrade DEHP preferentially.

Table 3. Kinetics parameters and Selectivity coefficient of MIP-TiO₂

Parameters	MIP-TiO ₂			TiO ₂		
	DEHP	DBP	DMP	DEHP	DBP	DMP
k (min ⁻¹)	0.0116	0.0056	0.0049	0.0079	0.0058	0.0048
$R(k_M/k_T)$	1.47	0.97	1.02	–	–	–
$\alpha(R_{target}/R_{non-target})$	–	1.52	1.44	–	–	–

3.5 Recycle of MIP-TiO₂

To investigate the reutilization of photocatalyst MIP-TiO₂, MIP-TiO₂ was used to degrade DEHP with an initial concentration of 5 mg/L for 3 h, centrifugally

separated, cleaned and dried, and then used to degrade DEHP(5 mg/L) again. The procedure mentioned above was repeated 5 times, and the photocatalytic efficiency for every time is shown in Fig. 10.

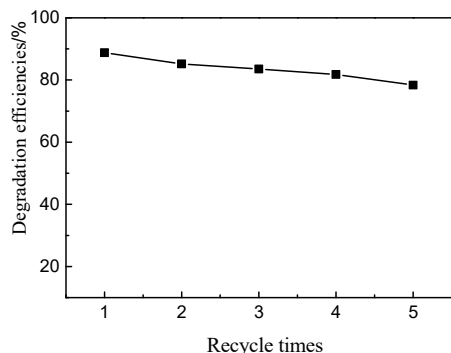


Fig. 10. Recycle of MIP-TiO₂

As seen in Fig. 10, the photocatalytic efficiency of DEHP is maintained between 88.8% and 78.4% during the reuse of MIP-TiO₂. Although the photocatalytic degradation efficiency of DEHP decreases slightly with the increasing in reuse of MIP-TiO₂, considering the photocatalytic efficiency decrease resulted from a certain loss of MIP-TiO₂ during solid-liquid separation, washing and drying, it is, therefore, concluded that MIP-TiO₂ is reusable.

4 Conclusions

MIP-TiO₂ was successfully synthesized with DEHP as template molecule, MAA as monomer and TiO₂ as support. MIP-TiO₂ retained the same anatase structure as TiO₂. Compared with TiO₂, MIP-TiO₂ exhibited enhanced light absorption, red-shifted absorption sideband and obviously specific recognition ability for DEHP. The imprinting factor of MIP-TiO₂ is 3.29, and the selectivity coefficient of MIP-TiO₂ toward DMP and DBP is 3.01 and 2.92, respectively. The DEHP molecularly imprinted polymer on the surface of TiO₂ effectively inhibited the photo-generated electron/hole recombination.

The photocatalytic degradation rate of DEP by MIP-TiO₂ is 1.5 times that of TiO₂. The photocatalytic degradation efficiency of DEHP with concentration of 5 mg/L was 89%. MIP-TiO₂ showed significantly photocatalytic selectivity for DEHP with selectivity coefficient of 1.52 and 1.44 for DEHP to DBP and DMP, respectively. The photocatalytic efficiency of DEHP was maintained in the range of 88.8% to 78.4% during being reused for 5 times.

Acknowledgements

This work was financially supported by the science and technology support projects of Zhangjiagnag City, China (Grant No. ZKS1510)

References

1. B. Bagó, Y. Martín, G. Mejía, F. Broto-Puig, *et al.* *Chemosphere*, **59**, 1191 (2005)
2. S. Huma, M. Najma, K. Hamayun, *et al.* *J. Chromatogr. A.*, **1247**, 125(2012)
3. T. J. Gray, S. D. Gangolli, *Environ. Health Perspect.*, **65**, 229(1986)
4. H. Fromme, T. Kuchler, T. Otto, *et al.* **36**, 1429 (2002)
5. J. Wang, Y.M. Luo, Y. Teng, *et al.* *Environ Pollut.*, **180**, 265 (2013)
6. M.M Abdel, U.J Rivera, R. Ocampo-PÉREZ, *et al.* *J. Environ. Manage.*, **109**, 164 (2012)
7. M. Julinová, R. Slavik. *J. Environ. Manage.*, **94**, 13 (2012)
8. H. Wei, Q. Ning, X.Z. Kong, *et al.* *Sci. Total Environ.*, **461**, 672 (2013)
9. X.L. Liu, P. Lv, G.X. Yao, *et al.* *Colloids Surf. A.* **441**, 420 (2014)
10. F. Deng, Y.X. Li, X.B. Luo, *et al.* *Colloids Surf. A.*, **395**, 183 (2012)
11. S. Anandan, N. Pugazhenthiran, T. Lana-Villarreal *et al.* *Chem. Eng. J.*, **231**, 182(2013)
12. K. Kabra, Chaudhary, R.L. Sawhney, *et al.* *Ind. Eng. Chem. Res.*, **43**, 7683 (2004)
13. X.Y. Tang, S.Y. Wang, Y. Yang, *et al.* *Chem. Eng. J.* **275**, 198 (2015)
14. W.Q. Sun, R. Tian, W.G. Zheng, *et al.* *Chinese J. Catal.*, **34**, 1589 (2013)
15. H. Li, G. Li, Z.P. Li, *et al.* *Appl. Surf. Sci.*, **264**, 644(2013)
16. X.L. Liu, P. Lv, G.X. Yao, *et al.* *Chem. Eng. J.* **217**, 398 (2013)
17. X. T. Shen, L. H. Zhu, N. Wang, *et al.* *Catal. Today.*, **225**, 164(2014)
18. Z. Q. Wang, X. Liu, W.Q. Li, *et al.* *Ceram. Int.*, **40**, 8863 (2014)
19. H. M. Zhao, Y. Chen, X. Quan, *et al.* *Chin. Sci. Bull.*, **52**, 1456 (2007)
20. B. Singh, N. Chauhan, V. Sharma. *Int. Eng. Chem. Res.*, **50**, 13742 (2011)
21. Y. Z. Yang, X. G. Liu, M. C. Guo, *et al.* *Colloids Surf. A.* **377**, 379 (2011)
22. F. J. Benitez, F. J. Real, J. L. Acero, *et al.* *J. Chem. Technol. Biotechnol.*, **84**, 1186(2009)
23. Z. Yang, F. Y. Chen*, Y. B. Tang, S. L. Li, *J. Chem. Soc. Pak.*, **37**, 939 (2015)
24. L. Yang, L. E. Yu, M. B. Ray. *Water Res.*, **42**, 3480(2008)